International Journal of Thermal Sciences 49 (2010) 290–301

Contents lists available at ScienceDirect

International Journal of Thermal Sciences

journal homepage: www.elsevier.com/locate/ijts

Formulation for predicting deposition velocity of particles in turbulence

M.C. Chiou [a,*], C.H. Chiu [a], H.S. Chen [b]

[a] Department of Vehicle Engineering, National Formosa University, 64 Wen-Hua Road, Yunlin 632, Taiwan
[b] Department of Material Science and Engineering, National Formosa University, Yunlin, Taiwan

ARTICLE INFO

Article history:
Received 13 April 2009
Received in revised form
8 July 2009
Accepted 17 July 2009
Available online 3 August 2009

Keywords:
Random surface renewal model
Eddy impaction
Particle inertia
Thermophoresis
Analytical equation
Deposition velocity

ABSTRACT

Relationships for the particle concentration and convection velocity profile has been obtained by the adaptation of the random surface renewal model [1–5] to the particle continuity and momentum equations of the nonisothermal turbulence boundary-layer flows; particle transport mechanisms of Brownian and turbulent diffusion, eddy impaction, particle inertia, and thermophoresis are included. This proposed model provides a useful framework for coupling these modeling parameters with analytical equation of the particle deposition velocity. The predictions obtained on the basis of this equation have been found to be in good agreement with experimental values of deposition velocity for fully-developed turbulent pipe flow.

1. Introduction

In the problem of particle deposition through a turbulent flow with fully developed boundary, the particles are generally assumed to be transported by turbulent diffusion except when they are very close to the wall where the turbulent eddy diffusivity vanishes. Early attempts to predict the rate of deposition onto plane surfaces assumed that particles traversed the viscous sublayer by molecular diffusion, which has been found to be satisfactory for the non-inertial particles. When τ_p^+ was increased, various investigators found that deposition rates were larger than predicted and presumed that the additional mechanisms of deposition had to be developed in order to explain this behaviour of deposition velocity. One of the most used calculation methods for the observed large increase in deposition velocity is the free-flight model [6–9]. The fundamental difference between different models of this type lies in prescribing the initial velocity that the particles possess at the distance where they effectively breaks away from the containing eddies and embarks on a free flight towards the wall. The first to offer a theoretical calculation method for observing large increase in deposition rates was based on a constant initial velocity, $0.9u^*$, and yielded reasonable agreement with deposition measurements for the intermediate particle relaxation times $0.1 < \tau_p^+ < 10$ [6]. The independence of initial velocity upon the position was questioned by arguing that that the initial velocity should be the same as the local rms fluctuation velocity of turbulent fluid, but the computed deposition velocities obtained on the basis of this assumption were lower by some two orders of magnitude than the measured values [7]. The calculations of deposition velocity obtained by another variation of free-flight model gave the results close to Friedlander and Johnstone predictions [8]. In order to improve the discrepancy of Davies's model, a new expression was taken into account for the particle eddy diffusivity, $\epsilon_p/\nu = \epsilon_p/\nu + \overline{v_f'^{+2}}\tau_p^+$ [9]. This model yielded reasonable agreement with deposition rate measurements for intermediate relaxation times, but poor agreement at high values where the measured deposition velocities has been found to be changed fairly to a slowly falling value with increasing the particle relaxation time [10,11]. This is primarily due to the additional factor $\overline{v_f'^{+2}}\tau_p^+$, which increases in an unbounded manner with relaxation time and does not reflect the difference between the particle and fluid fluctuation velocity. The deficiencies suggest that particle inertia does not solely manifest itself as an increased diffusivity in the boundary layer.

The previous paper [12] gave an alternative approach by adaptation of the surface rejuvenation model [13,14] to formulate the thermophoretic velocity and the particle concentration profiles in a nonisothermal turbulence flow with fully developed boundary layer. The behaviour of thermophoretic depositions within the average sublayer growth period obtained on the basis of this stochastic formulation stressed that the thermophoresis always

* Corresponding author.
E-mail address: achi@nfu.edu.tw (M.C. Chiou).

1290-0729/$ – see front matter © 2009 Elsevier Masson SAS. All rights reserved.
doi:10.1016/j.ijthermalsci.2009.07.016

Nomenclature

c	instantaneous particle concentration
C	mean particle concentration
c'	fluctuating particle concentration
C_c	Cunningham slip correction factor
C_f	Cunningham slip correction factor
c_p	specific heat at constant pressure
C_m	momentum exchange coefficient
C_s	thermal slip coefficient
C_t	temperature jump coefficient
d	tube diameter
D_b	Brownian diffusion
d_p	particle diameter
D_p	particle diffusion coefficient
f	friction factor
F_{th}	thermophoretic force
K_b	Boltzmann constant
K_g	thermal conductivity of carried gas
K_n	Knudsen number
K_p	thermal conductivity of particle
K_{th}	thermophoretic coefficient
N	particle mass flux
P	pressure
Pr	Prandtl number
p_τ	statistic distribution for τ
q	heat flux
r	tube radius
r_p	particle radius
Re	Reynolds number
$\Re_{Lf}(\tau)$	Lagrangian correlation coefficient
Sc	Schmidt number
T	mean temperature
T'	fluctuating temperature
u_f	instantaneous fluid velocity in axial direction
U_f	mean fluid velocity in axial direction
u'_f	fluctuating fluid velocity in axial direction
u_*	friction velocity
υ_f	instantaneous fluid velocity in radial direction
V_f	mean fluid velocity in radial direction
υ'_f	fluctuation fluid velocity in radial direction
υ_d	particle deposition velocity
υ_p	instantaneous particle velocity
V_p	mean particle velocity
υ'_p	fluctuating particle velocity
V_{pc}	particle convection velocity
V_{th}	thermophoretic velocity
x	distance along wall
y	distance from wall

Greek letters

α	thermal diffusivity
ρ	fluid density
ν	kinematic viscosity
σ_w	shear stress
μ	dynamical viscosity
ϵ_t	turbulent eddy viscosity
ϵ_m	turbulent eddy diffusivity
ϵ_p	particle eddy diffusivity
δ_m	maximum sublayer thickness
λ_p	mean free path
τ	sublayer growth period
τ_g	integral time scale
τ_p	particle relaxation time

Superscripts

$+$	Dimensionless parameters
$-$	average with respect to statistic distributions

Subscripts

∞	bulk stream conditions
w	wall conditions

remains an active transport mechanism right through the sublayer and that the small particles benefit most from this effect because with their low inertia they tend to follow the flow more closely. The predicted trend of average particle deposition velocities in an isothermal turbulence flow has been found to be in good agreement with both the Harriott technique [15] and the formulation proposed by [16]. However, as compared to the measured deposition velocities [10] that are generally accepted as one of most dependable data set, it can be inferred that the validity of this calculation scheme will be restricted in an intermediate range of particle relaxation time, and that the contradiction might be caused mainly by the absence of particle velocity fluctuations, which may be different from the fluid velocity fluctuations if the particle inertia is large. It should be noted that, on the other hand, the expression of analytical equations were limited to the determination of average transport properties in accordance with specified transport parameters because the order of Bessel function has to be a positive integer.

The acceleration of particles near the wall has been interpreted in the Eulerian framework by arguing that the particles with certain range of inertia moving against the wall-normal gradient in turbulent fluctuation intensity may cause them to trap into the low turbulence intensity regions, and that the wall-normal component of particle Reynolds stress in the regions enhanced by the interaction of particle inertia and the inhomogeneous turbulence flow plays an important role in the particle deposition mechanism [11,17–22]. The Eulerian computational methods of deposition have been developed by solving both the particle continuity and momentum equations, and represented considerable progress in the physical understanding of deposition processes. The absence of the use of the particle momentum equation in the previous paper [12] may therefore be its major weakness as well as the free-flight models, so that this work presents a model for calculating the deposition rate of particles in a simulate turbulence fluid field by analyzing both the particle continuity and momentum equations in connection with the random surface renewal model [1–5]. It is expected that the analytical approach obtained on the basis of this analysis is valid to quantitatively estimate the time-averaged particle transport rates for a wide range of particle sizes and that the physical trend of the comparable effects between the diffusive and convective flux on particle transport processes can be quantitatively revealed in some extent.

2. Average sublayer growth periods

The encounter of fluids with very different velocities forms a strong shear layer in a certain region above the wall and causes the energy dissipation by the small eddies as the agglomerate fluid lump disintegrated. An abrupt fluctuation caused by the rapidly growing violent instability of an exploded eddy with fluid possessing a high axial velocity penetrated into the viscous wall region not only leads to an acceleration of the low momentum fluid outward from the region

toward the shear layer, but also interacts with shear layer resulting in the chaotic motions that spread out in all directions. When the viscous interaction with the wall takes effect, a velocity gradient in the wall-ward fluid induced by the chaotic motions is gradually decelerated and gives rise to the establishment of a viscous motion progressively developing in a thin periodic fluid layer adjacent to the wall until a subsequent penetrating eddy. The visual flow studies have observed the continuously penetrating eddies leading to an unsteady flow in the regions close to the smooth tube wall and thus confirmed an existence of periodically thin wall layer immersed in the wall-bounded turbulent shear flows [23,24]. Based on these visualizations, the computational methods of the momentum, heat, and mass transfers in the wall-bounded turbulence flows have been developed on the basis of the sublayer approach concepts. These models stresses that, although the persistence of thin wall layer may not significantly influence the hydrodynamic characteristics of the locally developing boundary-layer flow, the influences of this thin wall layer on the heat or mass transfer cannot be ignored because these transfer processes, especially at very high Prandtl and Schmidt numbers, take place within a very thin layer adjacent to the wall [13–15,25,26].

In the turbulent shear flows with immersed particles, the momentum of turbulent fluid element is generally transported much more rapidly than the suspended particles. The local concentration differences relative to the quasi-random eddy variation of carrier fluid would change from a deterministic quantity to a quasi-random variable with the wall in a very short distance. Hence, the persistently-present turbulence structures in the close vicinity of the wall could be thought to govern particle transport towards the wall, i.e., deposition. Based on the random surface renewal model, the turbulent fluctuations imposed the mean shear on the boundary are associated with the interaction with an intermittently shear layer between turbulent and nonturbulent regions of the flow. They may not be the final mechanism for impaction on the surface because the kinematic constraints suppress the normal components of turbulent fluctuations on the boundary. However, an energetic exchange of turbulent eddy intermittently occurred in the viscous wall region has provided a conclusive demonstration of the dynamic nature in a very thin layer, where the most of production and dissipation of turbulent energy take place. Therefore, the additional stresses caused by turbulent fluctuation in the viscous wall region must be added to the ordinary viscous terms in the progressively developing sublayer.

In mathematical terms the velocity fluctuations superimposed on the main flow can be separated from other effects by decomposing the instantaneous parameters into a mean quantity and fluctuating component, i.e. $u_f = U_f + u'_f$ denoting the mean velocity of instantaneous velocity u in the axial direction by U_f and its velocity of fluctuation u', and $v_f = V_f + v'_f$ in the radial direction. Generally, the dimensions of the viscous wall boundary along the wall surface are very larger than its thickness, and the problem can be simplified by stipulating that the flow in the boundary layer of the conduit is regarded as an approximation to parallel flow because, as mentioned above, the maximum boundary thickness is considerably less than the characteristic diameter of the conduit. Based on this simplification, the dependence of the mean velocities in the main flow on the axial direction is very smaller than that on the radial direction, $V_f \ll U_f$ and $\partial/\partial x \ll \partial/\partial y$, and thus the shear stress σ_w in the turbulent boundary-layer flows may be approximated by

$$\sigma_w = \mu\frac{\partial U_f}{\partial y} - \rho\overline{u'_f v'_f}, \tag{1}$$

where y is the normal distance from the wall, μ the dynamical viscosity, and ρ the fluid density. The turbulent inertia composes the Newtonian viscous stress and the turbulent shear $\rho\overline{u'_f v'_f}$, where the mean value $\overline{u'_f v'_f}$ represents the turbulent element flux in the wall-normal direction as the fluid element transport. One attempts to model the fluctuation terms by assuming that the rate for a movement down the gradient of turbulent fluid element caused by turbulent shear is proportional to the magnitude of mean gradient and expresses as $-\rho\overline{u'_f v'_f} = \epsilon_m \partial U_f/\partial y$. If the effect of the turbulent fluctuations is taken into consideration by the turbulent eddy viscosity ϵ_t, the turbulent eddy diffusivity $\epsilon_m = \epsilon_t$ has been calculated by

$$\frac{\epsilon_t}{\nu} = y^{+(4-y^{+0.08})}\left[\frac{2.5\times 10^7}{\mathrm{Re}}\right]^{\frac{-y^+}{400+y^+}} \times 10^{-3} \text{ for all } y^+ = yu_*/\nu \text{ [7]}. \tag{2}$$

The characteristic features of sublayer approach concept are based on the assumptions that a rapidly decay penetration process is govern by an unsteady molecular transport in the viscous wall boundary-layer flows and that that the transformation of instantaneous properties into the lifetime of a single eddy can be achieved by substituting the residence time τ between successive eddies for the instantaneous contact time of a single eddy. Correspondingly, the boundary layer equation for unsteady momentum of an individual turbulence element near the wall with both mean and fluctuating quantities may be written as

$$\frac{\partial U_f}{\partial \tau} = -\frac{1}{\rho}\frac{dP}{dx} + (\nu + \epsilon_t)\frac{\partial^2 U_f}{\partial y^2}, \tag{3}$$

where the parameter dP/dx indicates the effect of the mean axial pressure gradient and ν the kinematic viscosity. Through the uniform diffusion substance in a turbulent element approaching the wall, the substitution for U_f by the bulk mean velocity u_∞ at the time just after the arrival of an eddy $\tau = 0$ has been found to be quite reasonable. The residence time τ between successive eddies has been considered as a statistical distribution varying with the corresponding distribution density function $p_\tau(\tau)$. It has been demonstrated that the forms of the distribution density function for the residence time τ over the surface did not appear greatly to affect calculated profile of the average transport properties [4,5,26–28]. For the convenient, the exponentially-distributed density function, $p_\tau(\tau) = (1/\overline{\tau})\exp(-\tau/\overline{\tau})$, proposed by [25] is taken account for predicting the transport properties during the average residence time $\overline{\tau}$ of all eddy lifetimes, which also establishes a measure of the average sublayer growth period. Consequently, the time dependency of an individual turbulence element can be transformed into the spatial variation of average time domain by multiplying each term of equation (3) with the exponentially-distributed density function $p_\tau(\tau)d\tau$ and then integrating with respect to the residence time τ, i.e.

$$\frac{d^2\overline{U}_f}{dy^2} - \frac{1}{(\nu+\epsilon_t)\overline{\tau}}\overline{U}_f = \frac{1}{\rho(\nu+\epsilon_t)}\frac{d\overline{P}}{dx} - \frac{1}{(\nu+\epsilon_t)\overline{\tau}}u_\infty, \tag{4}$$

where $\overline{U}_f = \int_0^\infty U_f p_\tau(\tau)d\tau$ and $\overline{P} = \int_0^\infty P p_\tau(\tau)d\tau$. The solution of equation (4) coupled with the boundary conditions of $\overline{U}_f = 0$ at $y = 0$ and $\overline{U}_f =$ finite as $y \to \infty$ leads to an expression for the time-averaged velocity profiles within the wall region of the form

$$\frac{\overline{U}_f}{u_\infty} = \left(1 - \frac{\overline{\tau}}{\rho u_\infty}\frac{d\overline{P}}{dx}\right)\left[1 - \exp\left(-\frac{y}{\sqrt{(\nu+\epsilon_t)\overline{\tau}}}\right)\right]. \tag{5}$$

For hydrodynamically fully developed flow through a circular tube of diameter d, the time-averaged flow profile can be written in terms of the friction velocity u^* from the pressure gradient $d\overline{P}/dx = -4\rho u_*^2/d$.

One of sublayer approach models proposed that the average growth period of viscous wall boundary layer relative to the outspread turbulence fluctuations is essentially determined by the value of maximum growth thickness [2,28]. Since the theory of viscous turbulent transition used does not admit a well-defined sublayer thickness, an alternative approach is taken into account by assuming that the Prandtl formula for the friction factor $f = 2(u_*/\overline{U}_f)^2$ proposed by [28] can reasonable be modified with the aid of the bulk mean fluid velocity $u_\infty^+ = (2/r^{+2})\int_0^{r^+}\overline{U}_f^+(r^+ - y^+)dy^+$ by putting $\overline{U}_f^+ = 0.99\,u_\infty^+$ and written as $f = 0.0757[\log(\mathrm{Re}/7.071)]^{-2}$, where the nondimensional tube radius $r^+ = ru_*/\nu = (\mathrm{Re}/2)\sqrt{f/2}$, $\overline{U}_f^+ = \overline{U}_f/u_*$, and $u_\infty^+ = u_\infty/u_*$. The nondimensional maximum growth thickness $\delta_m^+ = \delta u_*/\nu$ obtained on the basis of this assumption is expressed as a function of the friction factor and can be estimated for a given Reynolds number $\mathrm{Re} = 2u_\infty^+ r^+$. Subsequently, the formulation for nondimensional average sublayer growth period $\overline{\tau}^+ = u_*\sqrt{\overline{\tau}/\nu}$ can be derived from approximating the time-averaged velocity distributions profiles by logarithmic velocity profiles $\overline{U}_f^+ = 2.5\ln(y^+) + 5.5$ and also expressed in terms of the friction factor. It should be noted that the additional effect of turbulent eddy diffusivity ϵ_t in equation (5) induced by the turbulent fluctuations is not a constant but rather varies with the distance from the wall. As seen from Fig. 1, if the measurement of ϵ_t/ν is also simplified as corresponding with the maximum thickness, the variation of $\overline{\tau}^+$ with Re indicates that the period of the growth is increased with increased Reynolds number or equivalently the viscous turbulent transition near the wall is delayed. Although the magnitude of $\overline{\tau}^+$ slightly deviates from the visual flow observation that $\overline{\tau}^+$ is $14 \le \overline{\tau}^+ \le 17$ in the smooth tube flows for $2\times10^4 < \mathrm{Re} < 5.5\times10^4$ [24], its tendency is in basic agreement with experimental date obtained by [2] for fully developed tube flow conditions. The predicted trend is also shown for the case in which the effect of mean axial pressure gradient is neglected and the influence of the axial pressure gradient on $\overline{\tau}^+$ appears to be negligibly small for $\mathrm{Re} > 10^4$. This agrees with theoretical results that the axial pressure gradient on viscous sublayer becomes important for the deeper molecular penetration associate with low Reynolds number flow [12,13].

2.1. Thermophoretic velocities

In the wall-bounded turbulence shear flows with thermal intensity gradients, the heat transports of a nonisothermal fluid element intermittently moving to near the surface are analogous to its momentum. The effects of wall-normal turbulence on the instantaneous transport parameters can also be separated from other effects by decomposing the instantaneous temperature into a mean temperature T and a fluctuating temperature T'. Therefore, the heat flux q that consists of the molecular flux and the turbulent flux $\rho c_p\overline{T'v_f'}$ may be expressed as

$$q = -k\frac{\partial T}{\partial y} - \rho c_p\overline{T'v_f'}, \tag{6}$$

where k is the thermal conductivity and c_p the specific heat at constant pressure. Since the time mean values of the turbulent flux $\overline{u_f'v_f'}$ and $\overline{T'v_f'}$ arise from the same mechanism of mean fluid convection, the heat flux due to turbulent fluctuation may also be modelled by gradient diffusion and expressed as $\overline{T'v_f'} = -\epsilon_t\partial T/\partial y$.

Since the thermal boundary layer is thin, the temperature gradient across the viscous wall boundary layer in the y-direction is much larger than the gradient along it. When the dissipation is neglected, the unsteady energy transport of an individual turbulence element near the wall with both mean and fluctuating quantities can be approximated by substituting the residence time τ between successive eddies for the instantaneous contact time of a single eddy, and expressed by the form

$$\frac{\partial T}{\partial \tau} = (\alpha + \epsilon_t)\frac{\partial^2 T}{\partial y^2}, \tag{7}$$

where α thermal diffusivity. The transformation of time-dependent temperature distributions into the spatial variation of average time domain is analogous to that of the velocity distributions, and thus the time-averaged temperature distributions for the initial condition of $T = T_\infty$ at $\tau = 0$ can be written as

$$\frac{\partial^2\overline{T}}{\partial y^2} - \frac{1}{(\alpha+\epsilon_t)\overline{\tau}}\overline{T} = -\frac{1}{(\alpha+\epsilon_t)\overline{\tau}}T_\infty, \tag{8}$$

where $\overline{T} = \int_0^\infty Tp_\tau(\tau)d\tau$ and would be restricted to the boundary conditions of $\overline{T} = T_w$ at $y = 0$ and $\overline{T} =$ finite as $y \to \infty$. Once the variations of average sublayer growth period with the turbulent eddy intensity are known, the relative temperature distributions can be predicted by

$$\frac{\overline{T} - T_w}{T_\infty - T_w} = 1 - \exp\left(-\frac{y}{\sqrt{(\alpha+\epsilon_t)\overline{\tau}}}\right). \tag{9}$$

It has been accepted that a temperature gradient within a gas containing particles would give rise to the particle migrations towards the cooler fluid because the molecular bombardment of particles is more energetic on the hot side than on the cold side. A general formula for the thermophoretic force

$$F_{th} = -12\pi\mu v r_p C_s \frac{\frac{K_g}{K_p} + C_t K_n}{(1+3C_m K_n)\left(1+2\frac{K_g}{K_p}+2C_t K_n\right)}\frac{\nabla T}{T}, \tag{10}$$

proposed by [29], will be adopted to evaluated the thermal effects on particle transport processes over the entire range of Knudsen numbers. The thermophoretic force per unit particle mass is usually transformed into the corresponding thermophoretic velocity $\overline{V}_{th} = -(K_{th}\nu/\overline{T})\partial\overline{T}/\partial y$, where the thermophoretic coefficient K_{th} is characterized by the Knudsen number K_n and the ratio of thermal conductivity of the fluid K_g and the particle K_p. With the Cunningham slip correction factor [30]

$$C_f = 1 + K_n\left[1.257 + 0.4\exp\left(-\frac{1.1}{K_n}\right)\right], \tag{11}$$

the thermophoretic coefficient K_{th} is represented as

$$K_{th} = \frac{2C_s C_f\left(\frac{K_g}{K_p} + C_t K_n\right)}{(1+3C_s K_n)\left(1+2\frac{K_g}{K_p}+C_t K_n\right)}, \tag{12}$$

where $C_s = 1.147$ is the thermal slip coefficient, $C_t = 2.18$ the temperature jump coefficient, and $C_m = 1.146$ the momentum exchange coefficient [31]. The Knudsen number $K_n = \lambda_p/r_p$ is the ratio of mean free path λ_p to particle radius r_p. As a particle travels at its mean thermal velocity, the particle mean free path λ_p is calculated by $\lambda_p = \tau_p\sqrt{12K_bT/\pi^2\rho r_p^2}$ with Boltzmann constant $K_b = 1.38\times10^{-23}J/K$ and, incorporating the Cunningham correction

$$C_c = 1 + \frac{1}{Pd_p}\left[15.6 + 7.0\exp(-0.059Pd_p)\right] \tag{13}$$

with the absolute pressure P in kPa and the particle diameter d_p in μm, the particle relaxation time τ_p is calculated by $\tau_p = C_c\rho_p d_p^2/18\mu$, where ρ_p the particle density [32]. A constant thermophoretic coefficient $K_{th} \approx 0.55$ has been concluded to be applicable for the particles in transition regime $K_n \approx 1$ and free

molecule flow regime $K_n \gg 1$, which represents that the thermophoresis in the regions is independent of thermal conductivity ratio and has its largest effect [33]. It has been obtained that, when the particle size involved falls in the continuum regime $K_n \ll 1.0$, the effect of thermophoresis is significantly enhanced with reduced heat conductivity in particles because the thermophoretic coefficient K_{th} decreases continuously with increasing particle sizes [34]. This has been explained by considering that the thermophoretic mechanism for larger particles is subjected to the gas slipping along the nonuniformly heated particle surface, where the nonuniformity is stipulated by the temperature gradient of gas and strongly depends on the thermal conductivity of particles [35].

The calculated values of thermophoretic coefficient $K_{th} \approx 0.55282$ indicate that the particle sizes involved in the present model lie in the free molecule flow regime and come closer to the transition regime with the larger particles. Subsequently, the temperature distributions of equation (9) obtained on the basis of present analysis would be adapted to evaluate the thermophoretic effect in accordance with the nondimensional thermophoretic velocity $\overline{V}_{th}^{+} = \overline{V}_{th}/u_*$ of the form

$$\overline{V}_{th}^{+} = \frac{-K_{th}\frac{T_\infty - T_w}{T_\infty}}{\overline{\tau}^{+}\sqrt{\frac{1}{Pr}+\frac{\epsilon_t}{\nu}}\left[e^{\left(\frac{y^+}{\overline{\tau}^{+}\sqrt{\frac{1}{Pr}+\frac{\epsilon_t}{\nu}}}\right)} - \frac{T_\infty - T_w}{T_\infty}\right]}, \tag{14}$$

where Prandtl number $Pr = \nu/\alpha$. Since the thermophoretic velocity V_{th} represents an additional effect on the particle mass flux towards the wall as a result of a temperature gradient within a fluid containing particles, Fig. 2 reveals the dependence of thermophoretic velocity distributions upon the normalized particle relaxation time τ_p^+ for different Reynolds numbers to directly characterize the interaction of the particle inertia, the viscous drag resistance, and the thermophoretic drift mechanism.

The heat flux against the temperature gradient is dominated essentially by the molecular conduction and could be enhanced by the temperature fluctuation as a result of the wall turbulence fluctuation in a fluid eddy approaching to the wall. The calculations of thermophoretic velocity $\overline{V}_{th}^{+}$ at location of about one particle radius from the wall have its largest values for each τ_p^+ because the temperature fluctuation in the region very close to the wall is higher than elsewhere as well as the temperature gradient. The variation of calculated $\overline{V}_{th}^{+}$ becomes relatively insensitive to the change of τ_p^+ with increasing Reynolds number. This reveals that the temperature fluctuations in a fluid eddy approaching to the wall would result in distinct heat flux gradients with respect to the fluctuations of periodic sublayer. At high Reynolds number, the fluid is replaced at much lower frequency, the resistance within viscous sublayer drags the surrounding fluid and prevents the fluid from taking more heat, so that the effect of particle size is much less than the effect of thermal intensity gradient in the vicinity of the wall. It is shown that, however, the augmentation of $\overline{V}_{th}^{+}$ caused by thermal fluctuation intensity is more pronounced on the smaller particles than the larger particles. Considering the fact that, as the particle size increases, the value of Knudsen number decreases and shifts the thermal force mechanism toward the continuum regime where the effect of thermal intensity gradient in the vicinity of the wall is much less than the effect of particle size and the thermophoretic effect decreases with increasing particle size. Calculations are also shown for the case in which the effect of axial pressure gradient is neglected. A quite dramatic influence of axial pressure gradient on the on the thermophoresis is observed for each Reynolds number.

3. Governing equations for particle deposition

In general, the investigations of particle deposition mainly include incompressible fluid laden by spherical and dilute particles in the fully-developed turbulence boundary-layer flows. This means that the fluid motion is unaffected by the presence of the particles and that the collisions between particles can be neglected. If the density of the particle is considerably larger than the density of the carrier fluid, a number of external forces can also be neglected, such as gravity, electrical forces and Bassett's history terms. Therefore, neglecting the gravity and the lifting force, the viscous drag effect that acts on individual particles imposed by the surrounding fluid is assumed to be an important mechanism to induce the wallward particle motion as a consequence of the different velocities between particles and carrier fluid. In the case where there are no strong external forces that induce motion, the molecular diffusion becomes important for the particle migrations against the concentration gradient. When a temperature gradient is maintained, thermal diffusion contribution to the transport processes needs additionally to take into account.

Inside the wall-bounded shear layer, the concentration gradients of diffusing substance in a fluid eddy approaching to the wall is established, but the characteristic thickness of the concentration boundary layer at the interface is extremely thin in the case of immersed particles. Hence, the derivatives in y-direction are assumed to be much larger than in the other directions, and the unsteady equations for the particle mass balance and the particle transport in an individual turbulence element near the wall may be approximated by

$$\frac{\partial c}{\partial \tau} + \frac{\partial (c v_p)}{\partial y} = 0, \tag{15}$$

$$\frac{\partial (c v_p)}{\partial \tau} + \frac{\partial (c v_p v_p)}{\partial y} = \frac{c\left(v_f - v_p\right)}{\tau_p} - \frac{D_b}{\tau_p}\frac{\partial c}{\partial y} + \frac{c V_{th}}{\tau_p}, \tag{16}$$

where c denotes the instantaneous concentration of particles, and the instantaneous velocity v_p of particles is a consequence of the external force that acts on individual particles imposed by the surrounding fluid. The Brownian diffusion D_b for a rarefied gas effect

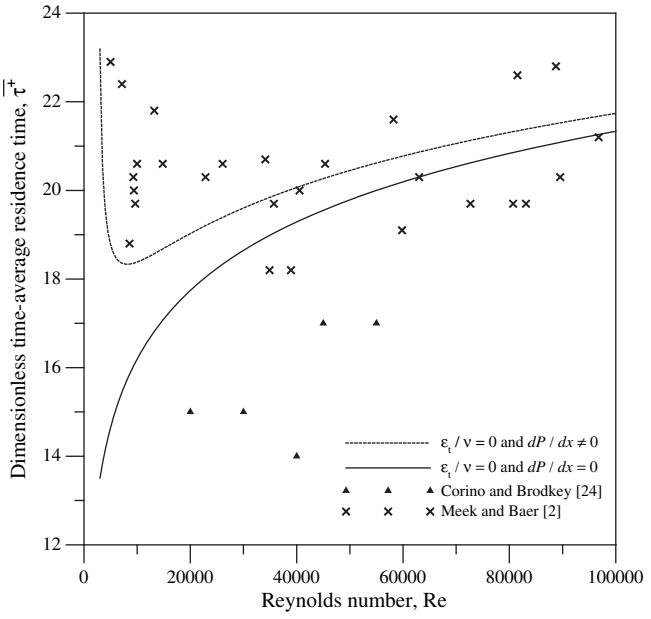

Fig. 1. Average sublayer growth period $\overline{\tau}^+$ as function of Reynolds number.

is calculated by $D_b = C_c K_b T/3\pi\mu d_p$ [32]. As mentioned early, the additional stresses associated with turbulent fluctuation can be separated from other mechanisms by decomposing the instantaneous parameters into a mean quantity and fluctuating component. Analogously, $c = C + c'$ and $\upsilon_p = V_p + \upsilon'_p$ denote the mean components of instantaneous properties c and υ_p in the wall-normal direction by C and V_p, and their fluctuation components c' and υ'_p. Applying these processes to the equations (15) and (16) the mean particle flux N of turbulent fluid element that intermittently move to near the wall can be written as $N = CV_p + \overline{c'\upsilon'_p}$. Since the time mean value of turbulent flux $\overline{c'\upsilon'_p}$ arises from the same mechanism of mean fluid convection, the particle mass flux due to the turbulent fluctuation may be simply modelled by the gradient diffusion, $\overline{c'\upsilon'_p} = -\epsilon_p \partial C/\partial y$, with the proportional constant of particle eddy diffusivity ϵ_p. Consequently, the particle conservation equations with both mean and fluctuating quantities might be approximate by

$$\frac{\partial C}{\partial \tau} = -\frac{\partial C V_p}{\partial y} + \epsilon_p \frac{\partial^2 C}{\partial y^2}, \tag{17}$$

$$\frac{\partial V_p}{\partial \tau} = -\frac{\partial \overline{\upsilon'^2_p}}{\partial y} - \frac{V_p}{\tau_p} - \frac{D_b}{\tau_p C}\frac{\partial C}{\partial y} + \frac{V_{th}}{\tau_p}. \tag{18}$$

3.1. Particle convection velocities

The particles with sufficient inertia moving against the sharp decay of turbulent intensity have been expected to possess higher deposition rates, and $\overline{\upsilon'^2_f}\tau_p^+$ in the equation for particle eddy diffusivity $\epsilon_p/\nu = \epsilon_t/\nu + \overline{\upsilon'^2_f}\tau_p^+$ was defined as an enhanced factor portraying the behaviour of higher deposition rates [9]. Relative to the experimental results [10], this model yielded reasonable agreement with deposition rate measurements for intermediate relaxation times, but poor agreement at high values. This is primarily due to the enhanced factor, which increases in an unbounded manner with relaxation time and does not reflect the difference between the particle and fluid velocity fluctuations.

In order to partly overcome this insufficiency, the present model incorporated the particle momentum equation in the analysis by considering that the particles are pushed by a gradient in the intensity of wall-normal velocity fluctuations and trapped in the viscous wall region, and that the fluctuating velocities of suspended particle and carrier fluid in the region are coupled through the balance between the convective acceleration and the viscous drag resistance. Based on the manner suggested by [19,20] and [36], the net particle flux is separated into the diffusive and convective components by defining $V_p = V_{pc} - (D_b/C)\partial C/\partial y + V_{th}$. With this simplification, the concentration dependent terms of the external forces imposed by the surrounding fluid are decomposed from the equation (18) and shifted into the mass conservation equation (17) through a modified form of the mean particle flux N

$$N = -(D_b + \epsilon_p)\frac{\partial C}{\partial y} + CV_{pc} + CV_{th}, \tag{19}$$

where the mean convective drift velocity of solid particles can thus be solved independently from the particle momentum equation

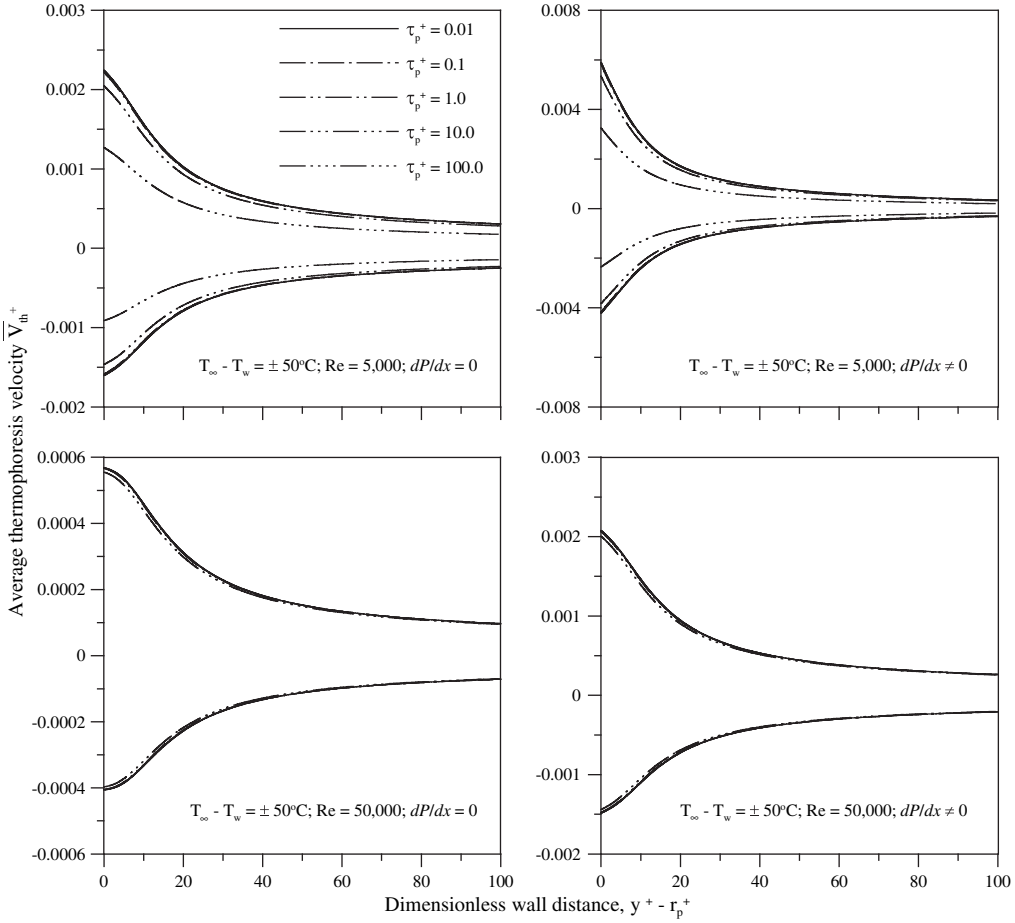

Fig. 2. Distribution of average thermophoresis velocity $\overline{V}_{th}^+$ relative to particle relaxation time τ_p^+ at fixed $K_g/K_p = 0.1$, $\rho_p/\rho_g = 1000$, and Pr = 0.708.

$$\frac{dV_{pc}}{d\tau}+\frac{V_{pc}}{\tau_p}=-\frac{d\overline{v_p'^2}}{dy}. \tag{20}$$

The gradient in turbulent fluctuation intensities at a sufficient distance away from the wall is negligibly small. The particle convective velocity gained by this intensity gradients may reasonably be neglected at the time just after the arrival of a turbulent eddy, $V_{pc}=0$ at $\tau=0$. Following the transformation of carrier fluid properties into the spatial variation of average time domain, the distributions of convective drift velocity $\overline{V}_{pc}^{+}=\overline{V}_{pc}/u_*=\int_0^\infty V_{pc}^{+}p_\tau(\tau)d\tau$ within the average sublayer growth period can be estimated by

$$\overline{V}_{pc}^{+}=-\tau_p^{+}\frac{d\overline{\overline{v_p'^{+2}}}}{dy^{+}}\left(1+\frac{\tau_p^{+}}{\tau_p^{+}+\overline{\tau}^{+2}}\right). \tag{21}$$

It is apparent that for the motion of fluid possessing a fixed wall-contact time $\overline{\tau}^{+}$ the important feature of convective drift mechanism on the transport processes is mainly emerged in both the gradient of time-average fluctuation velocity $\overline{v_p'^{+2}}=\int_0^\infty \overline{v_p'^{+2}}p_\tau(\tau)d\tau$ and the particle inertia. A linear differential equation for Reynolds normal stress of the particles in the presence of memory effect has been proposed by [21]. Based on the time mean values of the fluid and particle turbulence flux arising from the same mechanism of mean fluid convection, this equation may be reasonably modified by substituting the residence time τ of an individual eddy element for the instantaneous contact time and written as

$$\frac{dv_p'}{d\tau}+\frac{1}{\tau_p}v_p'=\frac{1}{\tau_p}v_f'. \tag{22}$$

From the Lagrangian correlation coefficient $\Re_{Lf}(\tau)=\exp(-\tau/\tau_g)=\overline{v_f'(0)v_f'(\tau)}/\overline{v_f'^2}$ of the fluid motion in the stationary homogeneous uniform flow [37], the solution of the mean fluctuation velocity of particles that satisfies the initial condition $v_p'=0$ at $\tau=0$, is expressed as

$$\overline{v_p'^2}(\tau)=\overline{v_p'^2}\left[1-2\exp\left(-\frac{\tau_g+\tau_p}{\tau_g\tau_p}\tau\right)+\exp\left(-\frac{2}{\tau_p}\tau\right)\right]. \tag{23}$$

where $\tau_g=\epsilon_t/\overline{v_f'^2}$ is integral time scale of the Lagrangian correlation. Simultaneously, within the average sublayer growth period a constitutive relation for the wall-normal fluctuation velocities of immersed particles and carrier fluid can be derived and expressed as

$$\overline{\overline{v_p'^{+2}}}=\overline{v_p'^{+2}}\left(1-\frac{2\tau_g^{+}\tau_p^{+}}{\overline{\tau}^{+2}\tau_g^{+}+\overline{\tau}^{+2}\tau_p^{+}+\tau_g^{+}\tau_p^{+}}+\frac{\tau_p^{+}}{2\overline{\tau}^{+2}+\tau_p^{+}}\right). \tag{24}$$

3.2. Particle deposition rates

The particle mass flux for the residence time of an individual eddy element in a nonisothermal fluid field has been established in terms of the Brownian and turbulent diffusion due to a gradient in the particle concentration, a convective drift due to the particle

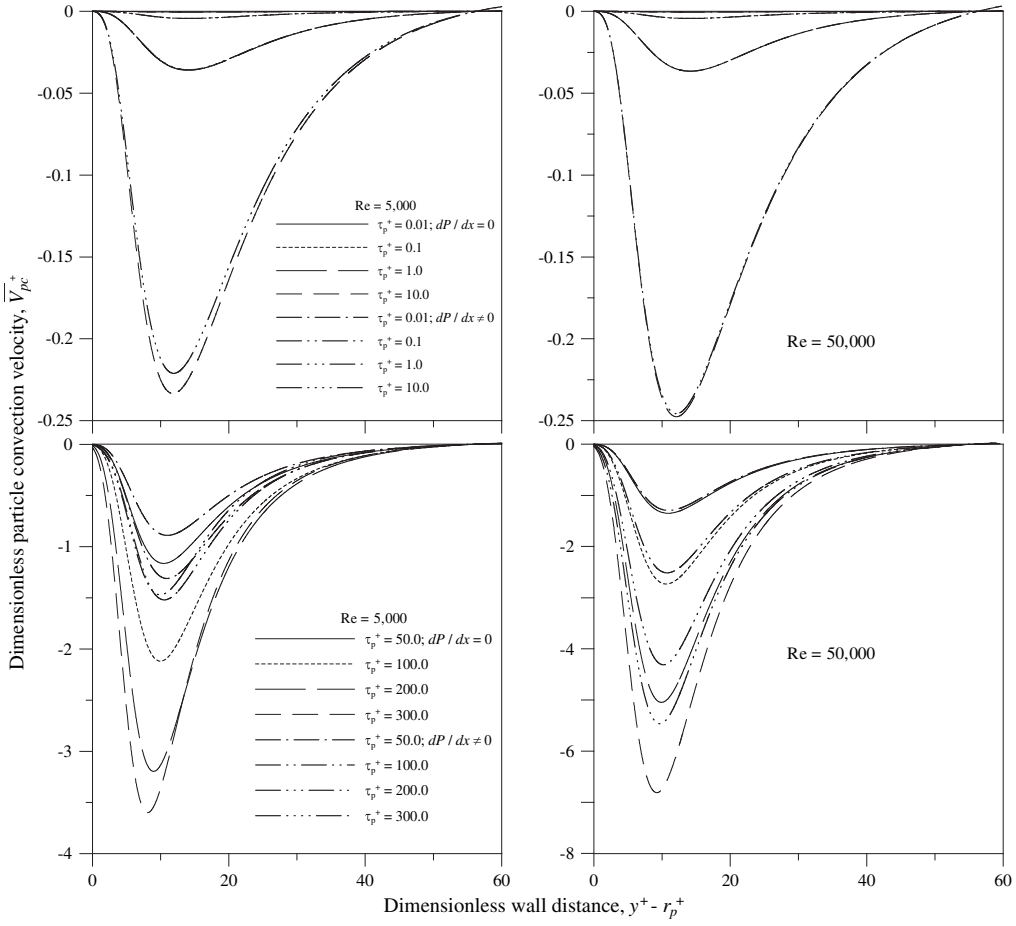

Fig. 3. Distribution of particle convection velocity $\overline{V}_{pc}^{+}$ relative to particle relaxation time τ_p^{+}.

inertia, and the thermal diffusion due to the temperature gradient. Hence, substituting equation (19) into equation (17) has the effect of shifting the diffusive terms into the mass conservation equation and leads to the relation

$$\frac{\partial C}{\partial \tau} = \frac{\partial}{\partial y}\left(D_p \frac{\partial C}{\partial y} - V_{th} C\right) - V_{pc}\frac{\partial C}{\partial y}, \tag{25}$$

where $D_p = D_B + \epsilon_p$ indicates a comparable effect between molecular diffusion and turbulent diffusivity of the particles. The mean concentration distribution of diffusing substance in a turbulent element approaching the wall is considered to be uniform, so that its magnitude at the time just after the arrival of an eddy $\tau = 0$ is set equal to the midstream fluid, $C = c_\infty$.

Same as the transformation of carrier fluid properties, the time dependency of particle concentration in an individual turbulence element near the wall can be transformed into the spatial variation of average time domain by multiplying each term of equation (25) with the exponentially-distributed density function $p_\tau(\tau)d\tau$ and then integrating with respect to the residence time τ. Subsequently, the distributions of particle concentration within the average sublayer growth period, $\overline{C}(y) = \int_0^\infty C(y,\tau)p_\tau(\tau)d\tau$, is considered to be restricted to the wall region by the boundary conditions of $C = c_w$ at $y = r_p$ and $C = c_\infty$ as $y \to \infty$, and thus the solution of time-averaged particle concentration can be obtained and expressed as the form

$$\overline{C}^+ = \frac{c_\infty - \overline{C}}{c_\infty - c_w} = \exp\left[-\frac{\sqrt{\left(4\frac{D_p}{\nu}\overline{\tau}^+ + 2\overline{V}_{th}^2\right) + \left(\overline{\tau}^+\overline{V}_{pc}^+\right)^2} - \overline{\tau}^+\left(\overline{V}_{th}^+ + \overline{V}_{pc}^+\right)}{2\frac{D_p}{\nu}\overline{\tau}^+}\left(y^+ - r_p^+\right)\right]. \tag{26}$$

Once the concentration dependent terms of the external forces imposed by the surrounding fluid in the equation for particle mass flux have been evaluated prior to the concentration boundary development, the concentration developments within the average sublayer growth period can be obtained. Consequently, the particle deposition velocity $\overline{v}_d^+ = v_d/u_* = N/u_*(c_\infty - c_w)$ can be predicted quantitatively by means of the form

$$\overline{v}_d^+ = \frac{\sqrt{\left(4\frac{D_p}{\nu} + \overline{\tau}^+ 2\overline{V}_{th}^+\right) + \left(\overline{\tau}^+ V_{pc}^+\right)^2} + \left(V_{th}^+ + \overline{V}_{pc}^+\right)\overline{\tau}^+}{2\overline{\tau}^+}. \tag{27}$$

4. Results and discussions

The isothermal experiment data of particle deposition from fully-developed turbulence pipe flow obtained by [10] are generally accepted as one of the most dependable data set and has been plotted against the simulated results of present approach model.

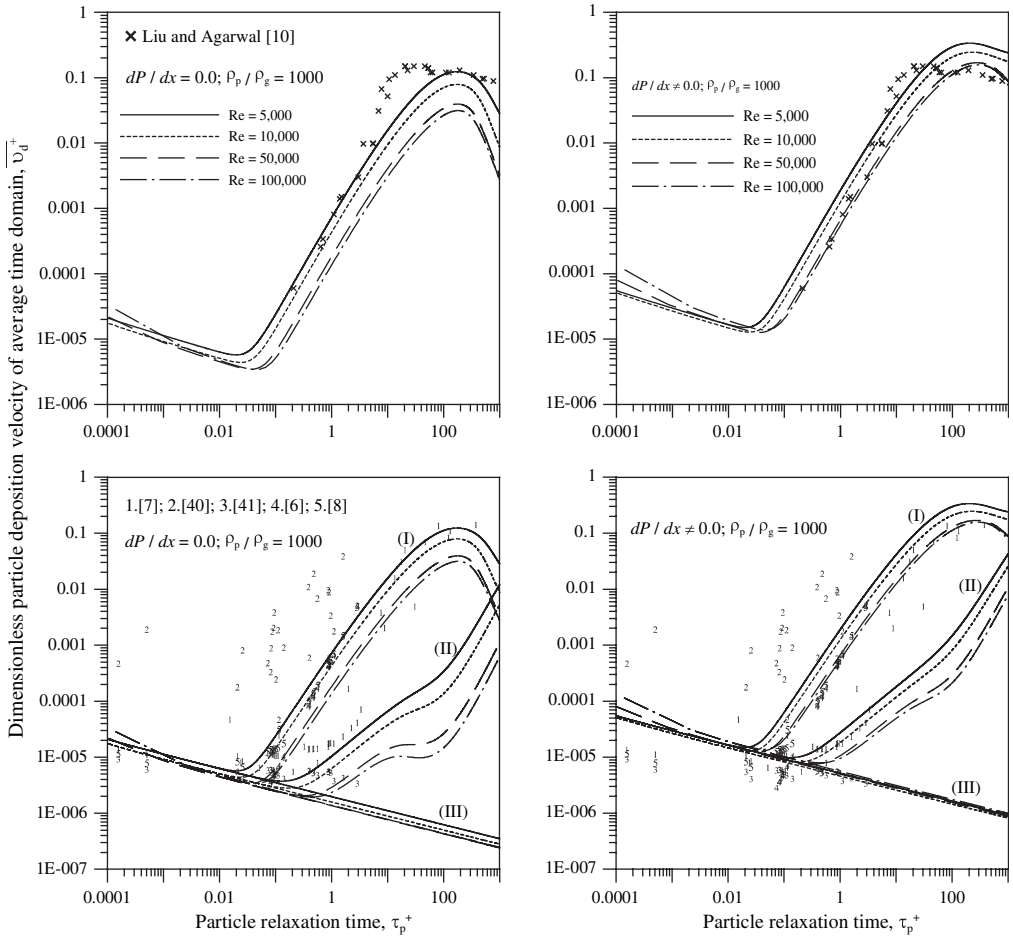

Fig. 4. Average deposition velocity $\overline{v}_d^+$ relative to τ_p^+ at different Reynolds numbers including mechanisms that dominate particle transport processes, (I) particle eddy diffusivity and convective drift [40] and [41] Doubt at $y^+ = r_p^+ + 0.9\tau_p^+$, and Brownian diffusion; (II) particle eddy diffusivity and convective drift at $y^+ = r_p^+$, and Brownian diffusion; (III) Brownian diffusion only.

Usually, the variation in measured deposition velocity $\overline{v}_d^+$ with particle relaxation time τ_p^+ has been divided into three distinct regimes [38], such as the turbulent diffusion regime where the particle transport to the wall is well represented by a gradient diffusion and $\overline{v}_d^+$ decreases monotonically with τ_p^+; the turbulent diffusion-eddy impaction regime where the particles acquire an impacting momentum towards the wall through interactions with turbulent eddies leading to a substantial increase in $\overline{v}_d^+$ with increasing τ_p^+; the particle inertia regime where the excessive particle inertia prevents particles from acquiring sufficient impacting momentum from the turbulence and results in a decline of $\overline{v}_d^+$ with increased τ_p^+.

The convective drift velocity $\overline{V}_{pc}^+$ of particles within the average sublayer growth period is calculated by substituting $y^+ = r_p^+ + 0.9\,\tau_p^+$ into $v_f'^+$ as the manner mentioned in [6], and solving the equation (24) for $\overline{v_p'^{+2}}$ and equation (21) by iteration. Fig. 3 emphasizes the fact that the damping of the turbulent properties by the wall is restricted to a very narrow region, especially for the particle velocity fluctuations. The gradient of these fluctuations is responsible for the predicted trend of $\overline{V}_{pc}^+$ profiles, which rise slowly from the main stream boundary to a maximum at a short distance close to the wall before dropping rapidly to zero at the wall. It is apparent that the peak position of $\overline{V}_{pc}^+$ profiles is dependent on the ability that the particles respond to the fluid velocity fluctuations. For $\tau_p^+ < 10$, the peak position of $\overline{V}_{pc}^+$ profiles is located at $y^+ \approx r_p^+ + 12$. This is because the low inertia particles closely follow the wallward fluid eddies and the velocity fluctuations of the particles and fluid are essentially the same, so that the kinematic constraint suppresses the wall-normal component of turbulent fluctuation intensity and forms an effective trap to prevent the particles from penetrating the viscous wall boundary layer to any great depth. For $\tau_p^+ > 10$, the peak position of $\overline{V}_{pc}^+$ profiles becomes sharper and closer to the wall with increasing particle diameter moderate as well as increasing the peak value. This stresses that, although high inertia particles respond poorly to the fluid turbulence, their induced velocities are more persistent than those of low inertia particles. The key feature of $\overline{V}_{pc}^+$ profiles obtained on the basis of the present calculation scheme is similar to that described in [21], the main difference being that non-equilibrium theory predicts the peak position $y^+ = 20$ due to the memory effect. However, it is important to note that the wall-normal gradient in particle velocity fluctuations induces an additional convection drift mechanism, which accelerates the particles toward the wall in a region within the peak position, but in the region beyond the peak position pushes the particles toward the main stream boundary.

In order to test the relative dependence of particle deposition velocity $\overline{v}_d^+$ upon the position where the particles respond to the fluctuating influences of fluid turbulence, two cases are considered; one is presumed to occur up to the distance $y^+ = r_p^+ + 0.9\tau_p^+$, and the other is located at about one particle radius from the wall. The deposition velocities calculated with two different locations are

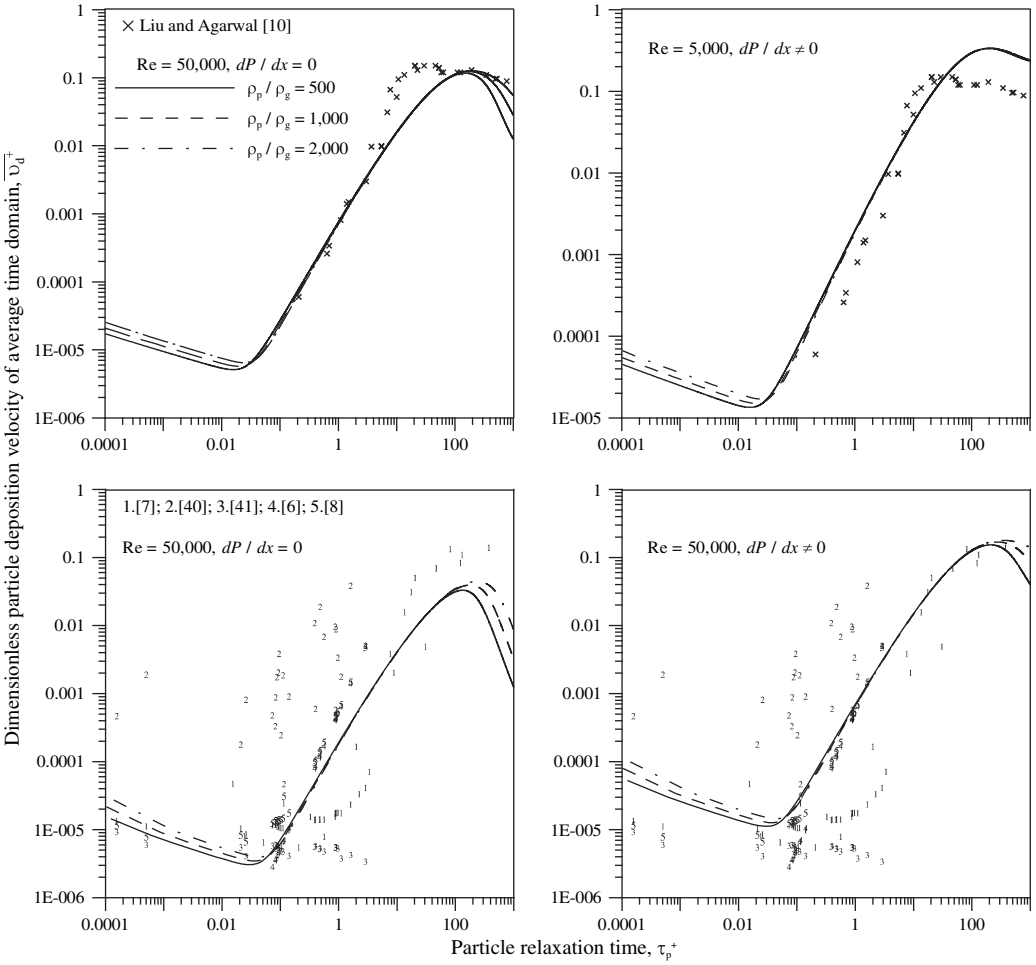

Fig. 5. Average deposition velocity $\overline{v}_d^+$ relative to τ_p^+ at different density ratios ρ_p/ρ_g including comparable effects of particle eddy diffusivity and convection drift [40] and [41] Doubt at $y^+ = r_p^+ + 0.9\tau_p^+$, and Brownian diffusion.

compared in Fig. 4 with existing theoretical and experimental data. The existing data are in reasonable agreement with predicted trend of $\overline{v}_d^+$ profiles using $y^+ = r_p^+ + 0.9\tau_p^+$, which gives reduced particle eddy diffusivity ϵ_p/ν with the particle diameter in the immediate vicinity of the deposition surfaces, when the particle sizes involved fall in the distance excesses its peak position. This can be postulated by considering that, as τ_p^+ increases, the particles are less able to respond faithfully to the fluid velocity fluctuations. The particle fluctuation velocity becomes progressively smaller than the fluid one, and consequently the strong gradient in the particle fluctuation intensities in the immediate vicinity of the wall enhances the convective flux through the increased $\overline{V}_{pc}^+$, but simultaneously reduces the diffusion flux through the decreased ϵ_p/ν. As a result of a net flux towards the wall, the reduction in the diffusive flux is smaller than the enhancement in the convective flux, so that the resulting diffusion towards the wall still remains higher than the diffusion towards the main stream boundary. This is usually termed particle inertia moderated regime, in which the deposition velocity $\overline{v}_d^+$ obtained by the present calculation scheme increases with decreasing τ_p^+, and the introduction of axial pressure gradient makes a substantial improvement in comparison with the experimental data. This tendency does not continue all the way to the small particles because the viscous drag resistances increases with decreasing particle diameter and usually balances the particle fluctuation intensity in the near-wall region. Therefore, the convective acceleration would progressively lose its importance with decreased τ_p^+, resulting in a decrease in the particle convection drift toward the wall in the turbulent diffusion-eddy impaction regime. In order to keep the net particle flux invariant for satisfying the continuity, the convective flux needs to be supplemented by a large diffusive flux which is achieved by the appropriate development of particle concentration profile close to the wall. The striking feature of this regime is that the deposition velocity decreases by three to four orders of magnitude with decreasing τ_p^+.

Curve (III) of Fig. 4 is calculated by directly correlating Brownian motion with the concentration gradient. Relative to curves (I) and (II), it is evidenced that, when the particle sizes involved fall in the turbulent diffusion regime, Fick's law of diffusion does provide a complete description of particle motion in the turbulent boundary layer. The deposition velocity $\overline{v}_d^+$ in this regime rises against with decreasing τ_p^+. In addition, the dependence of particle deposition upon the average sublayer growth period has been characterized by varying the Reynolds number. For hydrodynamically fully developed flow in a circular tube, an increase in Reynolds number results in an enhanced drag between adjacent fluid layers because of the effect of deep turbulence penetration. The predicted trend of $\overline{v}_d^+$ profiles shows that $\overline{v}_d^+$ decreases with increased Reynolds number in particle inertial moderated regime, goes through turbulent diffusion-eddy impaction regime, and then increases with increased Reynolds number in turbulent diffusion regime. This infers that the time-average particle flux related to the large scale turbulent structures in the vicinity of the wall decreases with increased the Reynolds number, except for small the particles because with their low inertia they tend to follow the

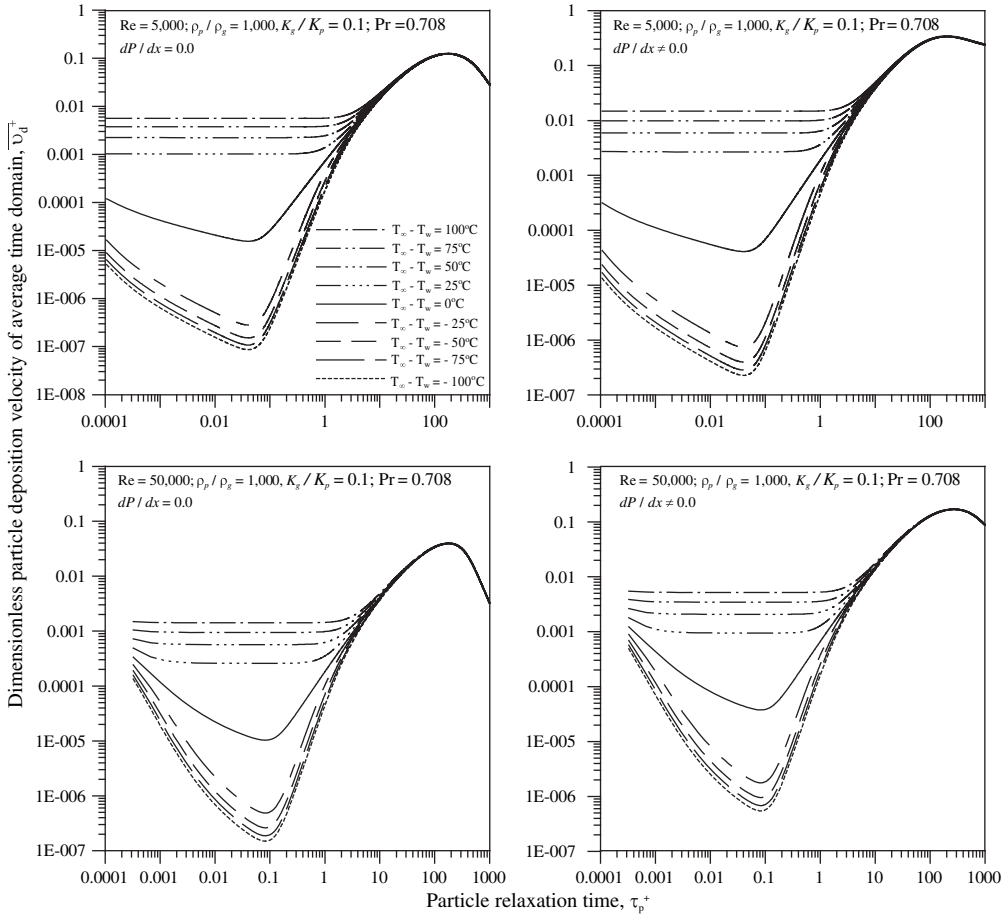

Fig. 6. Average deposition velocity $\overline{v}_d^+$ relative to τ_p^+ at different temperature differences $T_\infty - T_w$ including comparable effects of Brownian diffusion, particle eddy diffusivity and convection drift at $y^+ = r_p^+ + 0.9\tau_p^+$, and thermophoresis.

flow more closely. For this reason, the identical tendency of $\overline{v}_d^+$ verse τ_p^+ on different Reynolds numbers may not be expected as a general rule.

Fig. 5 demonstrates that the variations of $\overline{v}_d^+$ with τ_p^+ can also be compared with ρ_p/ρ_g for any Reynolds number. Generally, if there is a particle concentration gradient across the flow, then there exists a density gradient, which produces stable stratification and damps turbulence. The particle–turbulence interactions in the vicinity of the wall were investigated and the values of turbulent intensity were also evaluated from the corresponding Reynolds stress measurements [39]. The observed trend in Reynolds stress profiles indicates that the Reynolds stresses increase near the wall with increasing particle size, particle density and particle loading. The predicted trend of $\overline{v}_d^+$ profiles obtained by the present calculation scheme shows that the low inertia particles benefit most from the effect of increasing particle density ρ_p and that the enhancement is probably related to an enhancement of the Reynolds stresses increase near the wall as result increase in vertical component of turbulent fluctuation intensities. On the other hand, the deposition velocity $\overline{v}_d^+$ becomes relatively independent upon the density ratio ρ_p/ρ_g as the particle inertia takes effect. This is because the inertial effects originated from sharp decay of turbulent fluctuation intensities in outer region allow the discrete particles to maintain their high level of fluctuating intensity much close the wall, where $\overline{C}^+$ is of order unity everywhere.

When the variations in thermal intensity between colder and hotter region of the containing fluid are maintained, it has been shown in Fig. 2 that the magnitude of thermophoretic velocity within the average sublayer growth period has its largest value in the immediate vicinity of the wall and increases with decreased particle diameter. For the immersed particles in a nonisothermal fluid eddy approaching to the wall, the thermophoresis may be a significant drift mechanism for the particle transports against thermal intensity gradient as compared to other mechanisms. When Fig. 6 is referred to, it would be reasonable to point out that the thermal conductivity used, $K_g/K_p = 0.1$, represents rather low-conductivity particles (such as plastic particles in air) which helps emphasize the thermophoretic effect. It is apparent that the thermophoresis caused by thermal gradient near the wall has a very significant effect on the deposition velocity $\overline{v}_d^+$, particularly for small particles $\tau_p^+ < 0.1$, and that the magnitude of predicted $\overline{v}_d^+$ is somewhat higher for both non-zero axial pressure gradient and low Reynolds number. Considering that one particular area concerns accumulation of particles from gaseous suspensions onto cooled or heated solid objects, the thermophoresis is expected to play an important role there, because the gas molecules possessing high kinetic energy gained from the region of higher temperature strike the particles and the molecular bombardment of particles is more energetic on the hot side than on the cold side. The predicted results reveals clearly that the rates of particle deposit in the cold surface are increased by several orders of magnitude while the calculated results for the hot surface are counter to that of the cold surface. It should be noted that the larger gradient in fluid velocity fluctuations near the wall would make the larger particles maintain

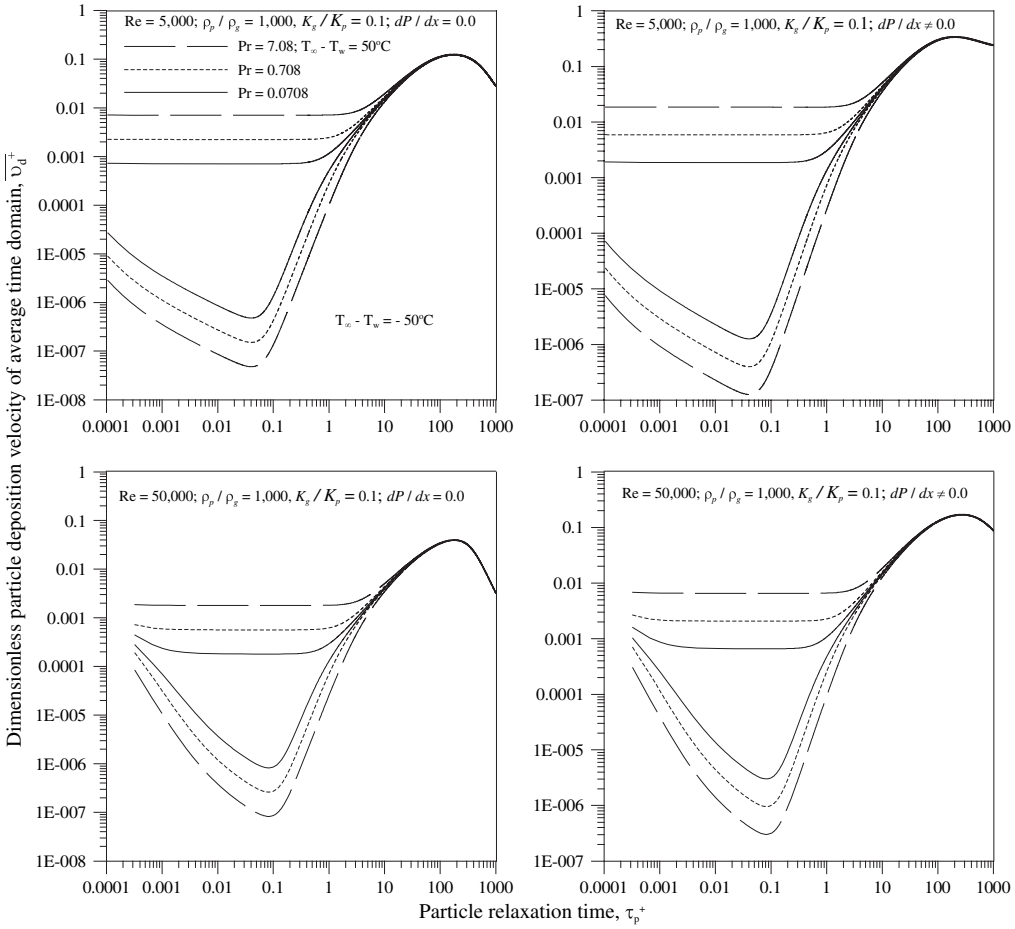

Fig. 7. Average deposition velocity $\overline{v}_d^+$ relative to τ_p^+ at different Prandtl numbers Pr including comparable effects of Brownian diffusion, particle eddy diffusivity and convection drift at $y^+ = r_p^+ + 0.9\tau_p^+$, and thermophoresis.

their high level of fluctuating intensity much closer to the wall, where the thermophoresis acts as a complementary mechanism to decrease the drag resistance against the net particle flux towards the cooled surface, and acts as an opposite effect in the case of heated surface, resulting in a substantial decrease in $\overline{v}_d^+$. Apparently, there is an interaction between thermophoresis and particle inertia in the region $0.1 < \tau_p^+ < 10$, and the inertial effects induced by the fluctuating intensity gradient always lower the increment of deposition velocity between temperature differences. It is shown that, however, for $\tau_p^+ > 10$ the thermophoresis has no effect on deposition velocity for the particular K_g/K_p ratio that was chosen and that for more-highly-conducting particles the dominance of inertial effects would arise for $\tau_p^+ < 10$.

Fig. 7 shows that the particle migration against the thermal gradient of surrounding fluid can also be viewed through the Prandtl number $\mathrm{Pr} = \nu/\alpha$, which acts as an important parameter for characterizing the relative importance of the momentum and energy transport in the nonisothermal turbulence flow fields. It can be seen that the characteristics of thermophoresis are very much dependent on its Prandtl number, and that the temperature fluctuations imposed on the fluctuating sublayer could cause an enhancement on the thermal force inside the relative quiescent viscous sublayer, resulting in the increase in thermophoretic deposition with increased Prandtl number. At low values of Pr, the thermal fluctuations adhere to the velocity fluctuations of the carrier fluid, so that the thermal transfer due to turbulence is restricted in the periodically developing boundary layer. Hence, the drag resistance of viscous sublayer will have significant effect on preventing the flow from taking more heat and thus reducing the overall transfer rate. When the Prandtl number Pr increases, the outer edge of growing sublayer is relatively farther from the wall than the penetration of the thermal wave during a growth cycle, so that the high thermal fluctuation maintains itself much closer to the deposition surface. Consequently, the heat transfer takes place within a very thin layer adjacent to the wall, where the difference of thermophoretic effects widens because of the deep penetration of higher energy eddies, which give rise to an increase in thermophoretic deposition velocity with increased Prandtl number. It is important to note that the changes in Prandtl number Pr for $\tau_p^+ > 10$ also cease to have any effect as well as varying the temperature difference.

5. Conclusions

The previous work [12] tried to capture the phenomena of deposition by solving the particle continuity equation alone, and demonstrated that a simple analysis method could predict the general behaviour of particle deposition. However, it is limited to eliminating the average particle transport coefficients in terms of unspecified parameters of the average residence time and approach distance. The present work has overcome this insufficiency by extending the random surface renewal mode to simultaneously solve the particle continuity and momentum equations. A useful framework for estimating the various transport mechanisms is established in the form of analytical equations. The solution of these equations agrees well with experimental values of particle deposition velocity for entire range of particle size.

References

[1] R. Nijsing, Predictions of momentum, heat and mass transfer in turbulent channel flow with aid of boundary layer growth-breakdown model, Warmeund Stoffubertragung 2 (1969) 65–86.
[2] R.L. Meek, A.D. Baer, The periodic viscous sublayer in turbulent flow, AIChE J. 16 (1970) 841–848.
[3] W.V. Pinczewski, S.A. Sideman, Model for mass (heat) transfer in turbulent flow, moderate and high Schmidt (Prandtl) numbers, Chem. Eng. Sci. 29 (1974) 1969–1976.
[4] J.M.H. Fortuin, E.E. Musschenga, P.J. Hamersma, Transfer processes in turbulent pipe flow described by the ERSR model, AIChE J. 38 (1992) 343–362.
[5] E.E. Musschenga, P.J. Hamersma, J.M.H. Fortuin, Momentum, heat and mass transfer in turbulent pipe flow: the extended random surface renewal model, Chem. Eng. Sci. 47 (1992) 343–362.
[6] S.K. Friedlander, H.F. Johnstone, Deposition of suspended particles from turbulent gas stream, Ind. Eng. Chem. 49 (1957) 1150–1156.
[7] C.N. Davies, Deposition of aerosol from turbulent flow through pipes, Proc. R. Soc. A289 (1966) 235–246.
[8] S.K. Beal, Deposition of particles in turbulent flow on channel or pipe walls, Nucl. Sci. Eng. 40 (1970) 1–11.
[9] B.Y.H. Liu, T.A. Illori, Inertial deposition of aerosol particles in turbulent pipe flow, in: ASME symposium on Flow Studies in Air and Water Pollution, Atlanta, Georgia, 1973, pp. 103–113.
[10] B.Y.H. Liu, J.K. Agarwal, Experimental observation of aerosol deposition in turbulent flow, J. Aerosol Sci. 5 (1974) 145–155.
[11] G.A. KAllio, M.W. Reeks, A numerical simulation of particle deposition in turbulent boundary layers, Int. J. Multiphase Flow 15 (1989) 433–446.
[12] C.H. Chiu, C.M. Wang, M.C. Chiou, Turbulent thermophoresis effect on particle transport processes, IJTS 45 (2006) 1238–1250.
[13] L.C. Thomas, The surface rejuvenation model of wall turbulence: inner laws for u^+ and T^+, Int. J. Heat Mass Transf. 23 (1980) 1099–1104.
[14] R. Rajagopal, L.C. Thomas, Adaptation of the stochastic formulation of the surface rejuvenation model to turbulent convection heat transfer, Chem. Eng. Sci. 29 (1974) 1639–1644.
[15] P. Harriott, A random eddy modification of the penetration theory, Chem. Eng. Sci. 17 (1962) 149–154.
[16] J.A. Bullin, A.E. Dukler, Random eddy models for surface renewal: formulation as a stochastic process, Chem. Eng. Sci. 27 (1972) 439–442.
[17] S.T. Johansen, The deposition of particles of vertical walls, Int. J. Multiphase Flow 17 (1991) 355–376.
[18] J.W. Brooke, T.J. Hanratty, J.B. McLaughlin, Free-flight mixing and deposition of aerosols, Phys. Fluids 6 (1994) 3404–3415.
[19] A. Guha, A unified Eulerian theory of turbulent deposition to smooth and rough surfaces, J. Aerosol Sci. 28 (8) (1997) 1517–1537.
[20] S.A. Slater, A.D. Leeming, J.B. Young, Particle deposition from two-dimensional turbulent gas flow, Int. J. Multiphase Flow 29 (2003) 721–750.
[21] M. Shin, D.S. Kim, J.W. Lee, Deposition of inertia-dominated particles inside a turbulent boundary layer, Int. J. Multiphase Flow 26 (2003) 892–926.
[22] S. Cerbelli, A. Giusti, A. Soldati, ADE approach to predicting dispersion of heavy particles in wall-bounded turbulence, Int. J. Multiphase Flow 27 (2001) 1861–1879.
[23] A.T. Popovich, R.L. Hummel, Experimental study of the viscous sublayer in turbulent pipe flow, AIChE J. 13 (1967) 854–860.
[24] E.R. Corino, R.S. Brodkey, A visual investigation of the wall region on turbulent flow, J. Fluid Mech. 37 (1969) 1–30.
[25] P.V. Danckwerts, Significance of liquid-film coefficients in gas absorption, Ind. Eng. Chem. 43 (1951) 1460–1467.
[26] T.J. Hanratty, Turbulent exchange of heat and momentum with a boundary, AIChE J. 2 (1956) 359–362.
[27] J.M.H. Fortuin, P.J. Klijn, Drag reduction and random surface renewal in turbulent pipe flow, Chem. Engng. Sci. 37 (1982) 611–623.
[28] S. Brocker, A new viscous sublayer influx (VSI) concept for near-wall turbulent momentum, heat and mass transfer, Rev. Gen. Therm. 37 (1998) 353–370.
[29] L. Talbot, R.K. Cheng, R.W. Schefer, D.R. Willis, Thermophoresis of particles in a heated boundary layer, J. Fluid Mech. 101 (1980) 737–758.
[30] S.H. Friedlander, Smoke, Dust and Haze-Fundamentals of Aerosol Behavior, Wiley, New York, 1977.
[31] G.K. Batcheler, C. Shen, Thermophoretic deposition of particles in gas flowing over cold surfaces, J. Colloid Interface Sci. 107 (1985) 21–37.
[32] W.C. Hinds, Aerosol Technology – Properties, Behavior, and Measurement of Airborne Particles, vol. 2, John Wiley & Sons. Inc., 1999.
[33] A. Messerer, R. Niessner, U. Poschl, Thermophoretic deposition of soot aerosol particles under experimental conditions relevant for modern diesel engine exhaust gas systems, J. Aerosol Sci. 34 (2003) 1009–1021.
[34] J.S. Chang, T. Ishii, S. Matsumura, S. Ono, S. Teii, Theory of aerosol particle thermal deposition on flat body in a variable property fluid, J. Aerosol Sci. 18 (1987) 619–621.
[35] S.P. Bakanov, Thermophoresis in gases at small Knudsen numbers, Aerosol Sci. Technol. 15 (1991) 77–92.
[36] L.I. Zaichik, V.M. Alipchenkov, Statistical models for predicting particle dispersion and preferential concentration in turbulent flows, Int. J. Heat Fluid Flow 26 (2005) 416–430.
[37] J.O. Hinze, Turbulence, vol. 2, McGraw-Hill Book Company, New York, 1975.
[38] M.W. Reeks, G. Skyrme, The dependence of particle deposition velocity on particle inertia in turbulent pipe flow, J. Aerosol Sci. 7 (1976) 485–495.
[39] M. Rashid, G. Hetsroni, S. Banerjee, Particle–turbulence interaction in a boundary layer, Int. J. Multiphase Flow 16 (1990) 935–949.
[40] T.L. Montgomery, M. Corn, Aerosol deposition in a pipe with turbulent airflow, J. Aerosol Sci. 1 (1970) 185–213.
[41] V.G. Levich, Physicochemical Hydrodynamics, Prentice-Hall, Englewood Clifts, New Jersey, 1972.